CORE
Metadata, citation and similar papers at core.ac.uk
Provided by Loughborough University Institutional Repository

Quantum design of ionic liquids for extreme chemical inertness, and a new theory of the glass transition

Stephen Fletcher, Victoria Jane Black, Iain Kirkpatrick, & Thomas Stephen Varley.

Department of Chemistry, Loughborough University, Ashby Road, Loughborough, Leicestershire LE11 3TU, UK.
E-mail: stephen.fletcher@lboro.ac.uk.

Received: 27 September 2012. Revised: 5 December 2012. Accepted: 6 December 2012. Published online: 3 January 2013.

© Springer-Verlag Berlin Heidelberg 2013

Dedication

Dedicated to Professor Alexander Milchev on the occasion of his 70th birthday.

Abstract

In many modern technologies (such as batteries and supercapacitors) there is a strong need for redox-stable ionic liquids. Experimentally, the stability of ionic liquids can be quantified by the voltage range over which electron tunneling does not occur, but so far quantum theory has not been applied systematically to this problem. Here we report the electrochemical reduction of a series of quaternary ammonium cations in the presence of bis(trifluoromethylsulfonyl)imide (TFSI) anions, and use non-adiabatic electron transfer theory to explicate the results. We find that increasing the chain length of the alkyl groups confers improved chemical inertness at all accessible temperatures. Simultaneously, decreasing the symmetry of the quaternary ammonium cations lowers the melting points of the corresponding ionic liquids, in two cases yielding highly inert solvents at room temperature. These are called hexyltriethylammonium bis(trifluoromethylsulfonyl)imide (HTE-TFSI) and butyltrimethylammonium bis(trifluoromethylsulfonyl)imide (BTM-TFSI). Indeed, the latter are two of the most redox-stable solvents in the history of electrochemistry.

To gain insight into their properties, very high precision electrical conductivity measurements have been carried out in the range +20°C to +190°C. In both cases the data conform to the Vogel-Tammann-Fulcher (VTF) equation with “six nines” precision ($R^2 > 0.999999$). The critical temperature for the onset of conductivity coincides with the glass transition temperature T_g. This is compelling evidence that ionic liquids are, in fact, softened glasses. Finally, by focusing on the previously unsuspected connection between the molecular degrees of freedom of ionic liquids

and their bulk conductivities, we are able to propose a new theory of the glass transition. This should have utility far beyond ionic liquids, in areas as diverse as glassy metals and polymer science.

Introduction

“Ionic liquids” are combinations of anions and cations that melt at temperatures lower than conventional molten salts. In optimal cases, they have high chemical stability and low vapor pressure, which means that they can be used as novel media for chemical reactions. Indeed, the dual prospects of long life and enhanced safety explain why ionic liquids are being widely mooted as “green” industrial solvents (i.e., environmentally benign alternatives to organic solvents). In the present work, we describe the rational design of ionic liquids for extreme chemical inertness.

A few materials (such as ethanolammonium nitrate, m.p. 52-55°C) that we would recognize today as ionic liquids were synthesized as far back as the 19th century [1]. However, it was not until the late 20th century that ionic liquids came into general prominence. First came the synthesis of inorganic chloroaluminates, then imidazolium and pyridinium chloroaluminates, and finally the vast range of compounds that we know today [2].

In terms of the industrial acceptance of ionic liquids, an important milestone was reached in 2002, when the BASIL process was introduced by BASF. [BASIL = Biphasic Acid Scavenging utilizing Ionic Liquids.] From this technology we learned that ionic liquids could be employed on an industrial scale. Today, the BASIL process is successfully used to synthesize alkoxyphenylphosphines, which are important intermediates in the production of printing inks and coatings [3].

At the time of writing (2012) the global chemical industry maintains a strong interest in ionic liquids, largely because they are potential alternatives to volatile organic compounds in chemical synthesis [4]. Uncontrolled atmospheric emissions, and widespread damage to the biosphere, have prompted international concern about conventional solvents. At the same time, there is a burgeoning demand for new media for homogeneous catalysis [5]. Ionic liquids represent a possible solution in both cases.

Of course, not all ionic liquids are “green” [6]. A few have potentially hazardous properties, such as high toxicity and/or low chemical stability, and the small scale of present-day production means that many are costly. Some also contain trace impurities. Common impurities include water, oxygen, and halide ions. Less common impurities include the hydrolysis products of water-sensitive ions, and even hydrogen fluoride [7, 8]. Whether such impurities are problematic or not depends on the experiments at hand, but for high-precision conductivity and voltammetry measurements the removal of water and oxygen is mandatory. In the present work, we found that water could be removed by high temperature evaporation (24h at 130°C). This process was assisted by the fact that the ionic liquids of interest to us were strongly hydrophobic.

The commercial availability of hydrophobic ionic liquids has opened up many new avenues of scientific enquiry. We note in particular the work of Appetecchi et al., who

screened a number of hydrophobic ionic liquids for use as electrolytes in supercapacitors and lithium batteries [9]. Their work involved a combination of bis(perfluoroalkylsulfonyl)imide anions and a variety of different cations. In particular, the authors measured the conductivity of the ethyl ammonium, *N*-ethyl-*N*-methyl imidazolium, and *N*-alkyl-*N*-methyl pyrrolidinium salts, and then demonstrated that the Vogel-Tammann-Fulcher equation [10-12] provided a good empirical fit to their data.

In its modern incarnation, the Vogel-Tammann-Fulcher equation takes the form

$$\kappa = A \exp\left(\frac{-B}{k_{\mathrm{B}}(T - T_0)}\right)$$

where κ is the conductivity $(\mathrm{S\,m^{-1}})$, and A, B, and T_0 are unknown constants. This expression is widely used to model conductivity data over finite ranges of temperature. Even though it lacks theoretical support, it has great utility as a fitting function because it successfully interpolates data in systems where the Arrhenius equation fails. In the present work, we derive the Vogel-Tammann-Fulcher equation from classical thermodynamics, and in doing so identify the unknown constants for the first time. In particular, we show that the parameter T_0 is actually the glass transition temperature T_{g}. Powerful evidence in favour of this interpretation is that values of T_0 obtained by high precision conductivity measurements coincide with values of T_{g} obtained by thermal analysis.

Besides the glass transition, another long-standing mystery has been the structure of the interface between an ionic liquid and an electrode surface [13]. It is now clear that the large sizes of the ions, and their lack of solvation, create very unusual effects. For example, at extreme electrode potentials, there can never be sufficient charge density in the first monolayer of adsorbed ions to sustain a sharp potential drop in the electrical double layer. It is logical, therefore, to postulate the existence of a compact layer of cations at extreme negative potentials, trapped by electrostriction at the electrode surface. Indeed, such a layer is revealed by the existence of electron tunnelling from the electrode surface into the unoccupied molecular orbitals of the cations. The precise structure of this electrostricted layer is, as yet, unknown: but we may safely conjecture that its reaction field involves contributions from ionic displacement, dipole orientation, and electronic polarization.

Beyond the first electrostricted layer, it has been suggested that a series of alternately-charged layers of ions may decay gradually into the bulk of solution. Direct observation of alternately-charged layers on a negatively charged Al_2O_3 (0001) sapphire surface was first reported by Mezger et al. using high-energy x-ray reflectivity measurements at 0.45 nm resolution [14]. The same authors adsorbed three different cations (1-butyl-3-methypyridinium, 1-hexyl-3-methylimidazolium, and tetrabutylammonium) and in all cases found pronounced molecular layering on top of the cation layer. A dense layer of ions on Au(111) has also been successfully imaged by STM, as reported by Waldmann et al. [15]. In a similar vein, Atkin et al., have performed STM /AFM and impedance studies of the interface between 1-butyl-1-methylpyrrolidinium tris(pentafluoroethyl)trifluorophosphate and Au(111), and found potential-dependent adsorbed multilayers of ions (as well as surface reconstruction of the substrate) [16]. Lastly, Roling et al. have carried out impedance studies on the same system, and found evidence of both fast and slow capacitive

charging processes [17]. These results emphasize the importance of allowing sufficient time (many seconds) for these interfacial systems to equilibrate.

From the cited works it is clear that there are drastic deviations from the classic Gouy-Chapman model of the double layer in the case of ionic liquids, and possibly very slow equilibration times too. In addition to these phenomena, we here report a strong decoupling of faradaic and capacitive charging phenomena. Decoupling occurs because electron tunnelling (which is very short-range) is dominated by the first layer of electrostricted counter ions, while double layer charging (which is very long-range) is affected by all the layers that are present.

In passing, we remark that the very short range of electron tunnelling (typically a few hundred picometers) also explains why scanning tunnelling microscopy resolves only the top layer of atoms on a solid surface, and why single monolayers of insulators are able to inhibit electrochemical reactions.

In parallel with experiments, the theory of double layers in ionic liquids has also developed rapidly in recent years. In 2007 Kilic et al. made the interesting prediction that the differential capacitance of electrodes might vary non-monotonically with the applied voltage [18]. Around the same time, Fedorov and Kornyshev carried out computer simulations which predicted that the double layer capacitance should be strongly affected by the physical arrangement of the ions and the complex structure of the force fields acting between them [19]. More recently, Paek et al. performed a computational study of the interfacial structure and capacitance of 1-butyl-3-methylimidazolium hexafluorophosphate on graphene, and found (in agreement with experiments on metals) that the cations accumulated in a dense layer immediately adjacent to the negative electrode, with alternately-charged layers on top [20].

Definition of Ionic Liquid

Lastly, in light of our own studies over very wide ranges of temperature, we feel compelled to revise the definition of an ionic liquid. Currently, all the literature definitions of “ionic liquid” employ the boiling point of water as a reference temperature. For example, one typical definition reads: “Ionic liquids are ionic compounds which are liquid below 100°C” [21]. Definitions of this kind, however, are arbitrarily restrictive, and it is difficult to understand how they arose in the first place. They pay scant regard to the fact that some ionic liquids survive indefinitely at temperatures >130°C, while others occur as mesomorphic (liquid crystalline) phases at room temperature [22, 23, 24]. Indeed, some ionic liquids (such as those used in the present work) survive brief excursions to 350°C (the temperature at which the pyrolysis of many molecular compounds begins [25]). Furthermore, the standard definition also omits any mention of the fact that conventional solvents are absent. To resolve these difficulties, we suggest the following revised definition:

☐ “Ionic liquids” are solvent-free combinations of anions and cations that display at least one liquid-like phase below 350°C.

This definition is accurate, and is fully consistent with the diverse behaviours of ionic liquids described in the scientific literature. It is also consistent with the definitions in the IUPAC “Gold Book” [26]. The temperature of 350°C is not fundamental, but it

does represent an empirical upper limit beyond which the thermolysis of molecular ions (i.e. the un-catalysed cleavage of one or more covalent bonds) is almost certain.

In the special case of room temperature ionic liquids, the revised definition becomes:

☐ "Room Temperature Ionic liquids" (RTILs) are solvent-free combinations of anions and cations that exist in a liquid-like phase at 25°C.

Experimental

Ionic liquids (>98 % purity) were synthesized on request by Io-li-tec (Ionic Liquid Technologies, Germany) and the purity confirmed by C-13 nmr. All ionic liquids were dried at 130°C for 24 h before use. **Voltammetry measurements** were performed in pyrex cells at 140 ºC. Working electrodes were glassy carbon disks (d = 3.0 mm) press fitted into glass-filled Teflon. Counter electrodes were fabricated in-house from Aldrich platinum gauze, 99.9%, 52 mesh (CAS 7440-06-4) and were machined into flags approximately 4 cm^2.

Ag|AgCl pseudo-reference half-cells were prepared in-house before use. High purity Ag wire (Johnson-Matthey, Stoke-on-Trent, UK (99.99%)), d = 1 mm, l = 10 cm) was abraded with emery paper, rinsed with deionized (millipore) water, and dried prior to immersion in ionic liquid. The Ag wire was then cycled voltammetrically in 0.5 M NaCl(aq) before being plated with silver chloride at +0.8 V versus an SCE reference half cell (60 s). This coated wire was then immersed in a given ionic liquid to create a "mixed" Ag|AgCl|($TFSI^-$) reference half-cell. As with a reported Ag|Ag^+|($TFSI^-$) reference half-cell [27], a stable reference potential was obtained, and liquid junction potentials between different quaternary ammonium bis(trifluoromethylsulfonyl)imide ionic liquids could readily be measured and were found to be less than 4 mV in all cases. This was well within tolerance for present purposes.

Voltammograms were recorded using an Autolab PGSTAT 20 potentiostat (ECO Chemie, Utrecht, Netherlands). **Conductivity measurements** were carried out in pyrex cells by means of platinized platinum conductivity probes (027-013, Jenway, UK). A digital thermometer (P755-Log, Dostmann Electronic, Wertheim, Germany) and a glass fiber flexible stirrer were also inserted into each test cell. Typically, the temperature was cycled repeatedly at 0.1 K min^{-1} between a lower temperature just above the melting point of the ionic liquid, and an upper temperature of 190ºC. The temperature was measured within ±0.01ºC, and impedance (Z), phase angle (ϕ), resistance (R), and capacitance (C) values were recorded every two seconds using a Precision Component Analyser (6430 A, Wayne-Kerr, UK). Calibration was against 0.01 M KCl, 1413 µS cm^{-1}, 25 ºC.

High purity nitrogen was delivered into the test cell via a drying trap, and stirring of samples was achieved by means of a flexible rotating glass fibre brush. During long-term measurements, the cell was hermetically sealed. In all reported experiments, residual water concentrations were decreased below the level of detection of cyclic

voltammetry. As a cross-check, voltammograms were routinely compared with those obtained after addition of hygroscopic fumed silica (to scavenge traces of water). No differences were observed. Throughout the present work, residual oxygen concentrations were also scrupulously minimized. In all cases dry nitrogen flushing was carried out until the oxygen reduction reaction was undetectable electrochemically. Any remaining impurities were also found to be below the level of detection by thermal analysis, by C-13 nmr, and by IR/visible spectrometry. Finally, to avoid surface reconstruction and other surface-specific effects, glassy carbon was selected as the electrode material for all interfacial voltammetric measurements.

Voltammetry Results

In order to study the rates of electron tunneling in a systematic way, we focused on the set of ionic liquids listed in **Table 1**. Their generic structure is shown in **Fig. 1**. The bis(trifluoromethylsulfonyl)imide anions ($TFSI^-$) are negatively charged, and hence are repelled from electrodes at high negative potentials. Conversely, the quaternary ammonium cations (R_4N^+) are positively charged, and hence are attracted to electrodes at high negative potentials. At close range (<1.4 nm) the nitrogen centers become the target of electron attack.

Table 1. Ionic liquids based on quaternary ammonium cations and bis(trifluoromethylsulfonyl)imide anions.

Common Name	Empirical formula	mp (°C)	Cation Radius (pm) [32]
Tetramethylammonium bis(trifluoromethylsulfonyl)imide	$[(CH_3)_4N+][(SO_2CF_3)_2N-]$	133	292
Tetraethylammonium bis(trifluoromethylsulfonyl)imide	$[(C_2H_5)_4N+][(SO_2CF_3)_2N-]$	109	347
Tetrapropylammonium bis(trifluoromethylsulfonyl)imide	$[(n\text{-}C_3H_7)_4N+][(SO_2CF_3)_2N-]$	105	390
Tetrabutylammonium bis(trifluoromethylsulfonyl)imide	$[(n\text{-}C_4H_9)_4N+][(SO_2CF_3)_2N-]$	96	424
Butyltrimethylammonium bis(trifluoromethylsulfonyl)imide	$[(n\text{-}C_4H_9)(CH_3)_3N+][(SO_2CF_3)_2N-]$	11 (19 [28])	336
Hexyltriethylammonium bis(trifluoromethylsulfonyl)imide	$[(n\text{-}C_6H_{17})(C_2H_5)_3N+][(SO_2CF_3)_2N-]$	5 (20 [29])	391
Methyltrioctylammonium bis(trifluoromethylsulfonyl)imide	$[CH_3\ (C_8H_{23})_3N+][(SO_2CF_3)_2N-]$	−70 [30,31] (?)	489

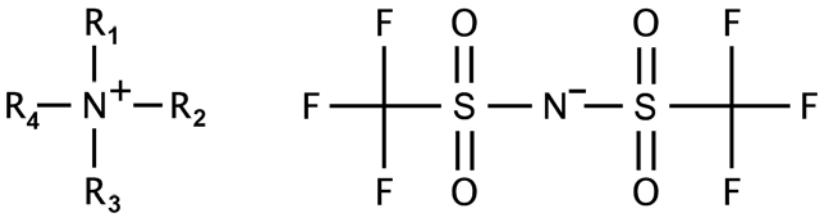

Fig. 1. The generic structures of the quaternary ammonium bis(trifluoromethylsulfonyl)imide ionic liquids studied in the present work.

In interfacial electrochemistry, electron transfer typically takes place by quantum tunneling of an electron from an occupied state near the Fermi energy of the electrode into an unoccupied state of the reactant molecule. Unfortunately, a complete analytical solution for the rate of this quantum tunneling process is impossible to obtain. This is because the Schrödinger equation is insoluble for all cases where an electron moves under the influence of more than one atomic nucleus, as in electron transfer. Nevertheless, some approximate results have been established, the most recent of which is due to Fletcher [33]. This takes the form

$$k_{\mathrm{et}} = \frac{2\pi}{\hbar}|H'|^2 S_{\mathrm{DA}}^2 \frac{1}{\sqrt{4\pi\lambda k_{\mathrm{B}} T}} \exp\left(\frac{-(\lambda + \Delta G^0)^2}{4\lambda k_{\mathrm{B}} T}\right) \tag{1}$$

Here k_{et} is the rate of electron transfer (s^{-1}), $\hbar$ is the reduced Planck constant (1.054×10^{-34} J s), H' is a constant (dimensions of energy) related to the electronic coupling matrix element between a single electron donor and a single electron acceptor, S_{DA} is the overlap integral (i.e. the extent of orbital overlap between the donor species and the acceptor species), λ is the reorganization energy (J), k_{B} is the Boltzmann constant (1.38×10^{-23} J K^{-1}), T is absolute temperature and ΔG^0 is the difference in Gibbs energy between the reactant and the product. Equation (1) is identical to the Levich-Dogonadze result [34] except that the overlap integral now appears explicitly in the pre-exponential term. In Dirac notation, the overlap integral is

$$S_{\mathrm{DA}} = \langle \psi_{\mathrm{D}} | \psi_{\mathrm{A}} \rangle \tag{2}$$

where ψ_{D} and ψ_{A} are the wavefunctions of the donor and acceptor orbitals. If the orbitals are Slater-type, as we expect, then S_{DA} should behave like

$$S_{\mathrm{DA}} = \alpha x^{\beta} \exp(-\gamma x) \tag{3}$$

and so the interfacial rate of electron transfer should decay sharply with increasing donor-acceptor distance x. (Here α, β and γ are constants defined in the original paper [35].)

Fig. 2 shows experimental Tafel plots for the electrochemical reduction of the four symmetrical tetraalkylammonium cations listed in **Table 1**. The data were obtained at a glassy carbon electrode at 140°C. The observed Tafel slopes (expressed in mV decade^{-1}) are tetramethyl 333, tetraethyl 258, tetrapropyl 248, and tetrabutyl 305, and conform to no standard mechanism. However, extrapolation of the current-voltage curves to *E* = −3.0 V allows the various rates of electron tunneling to be plotted as a function of ionic radius (**Fig. 2**), and we find that a single exponential

function is sufficient to fit the data with a quantum tunneling decay constant γ of 18 nm^{-1}. This agrees well with the data of Moser et al. [36, 37] who observed quantum tunneling decay constants of approximately 14 nm^{-1} for intra-protein electron transfer in a variety of biological systems. In the present work, it is evident that the ascent of the homologous series *methyl-, ethyl-, propyl-, butyl-,* ... causes a systematic decrease in the electron tunneling probability into the nitrogen center of the tetra-alkylammonium ions. As a result, tetra-butylammonium bis(trifluoromethylsulfonyl)imide has outstanding resistance towards electrochemical reduction. Hereafter, we refer to the structural inhibition of electron tunneling in potentially electroactive species as “quantum inertness”.

Despite the quantum inertness of tetra-butylammonium bis(trifluoromethylsulfonyl)imide, its melting point (96°C) is nevertheless too high for many industrial applications. The question therefore arises: can an ionic liquid be found that possesses quantum inertness at room temperature? As noted by Welton more than ten years ago, there is no reliable way to predict the precise melting point of organic salts [38]. However, the search can be accelerated by exploiting the fact that decreasing the symmetry of a component ion frequently decreases the melting point of the resulting ionic liquid [39]. Based on this insight, we recently performed differential scanning calorimetry on a series of asymmetric cation salts of the bis(trifluoromethylsulfonyl)imide anion, and can now confirm that butyltrimethylammonium bis(trifluoromethylsulfonyl)imide and hexyltriethylammonium bis(trifluoromethylsulfonyl)imide both have melting points below room temperature (**Table 1**). Thus, both of these compounds can be used as “quantum-inert” ionic liquids at room temperature. Their voltammograms are shown in **Fig. 3**. The voltage stability windows of each electrode, >3.5 volts wide, are among the widest yet reported. In associated work, we have found that very low temperatures can be accessed by using multiple long chain alkyl moieties such as methyl trioctyl groups although the resulting liquids tend to be very viscous due to chain entanglement.

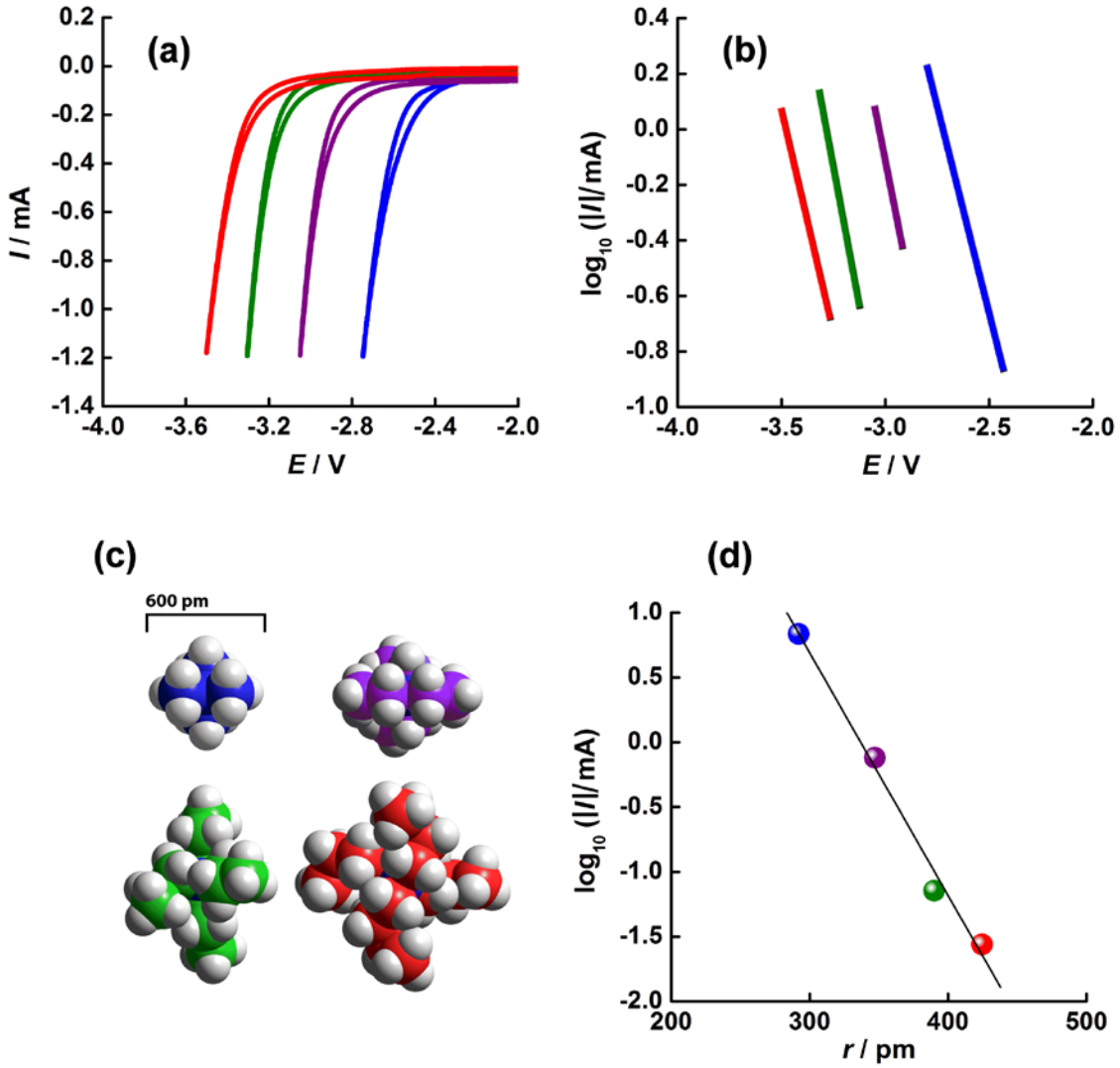

Fig. 2. Quantum Tunneling in Ionic Liquids.

(a) Cyclic voltammograms (superimposed) showing the cathodic reduction of four different tetraalkylammonium ions. The ions were; tetramethyl (blue), tetraethyl (purple), tetrapropyl (green), and tetrabutyl (red). In all cases the anion was bis(trifluoromethylsulfonyl)imide. The working electrode was a glassy carbon disk (d = 3.0 mm) press-fitted into a glass-filled Teflon shroud. The voltammetry was carried out in a thermostat-controlled electrochemical cell at 140°C. Scan rate 100 mV s^{-1}. The reference half-cell was Ag|AgCl|($TFSI^-$).

(b) Tafel plots for the electrochemical reduction of the four symmetrical tetraalkylammonium ions. From right to left the cations are tetramethylammonium, tetraethylammonium, tetrapropylammonium, and tetrabutylammonium.

(c) 3D Images created using the computer program Hyperchem (Hypercube Inc., Gainesville, FL, USA). The equivalent spherical radii of cations were computed using Stewart's semi-empirical (PM3) method [32].

(d) Decay of electron tunneling probability as a function of ionic radius for the series of symmetric tetraalkylammonium ions. Note the sensitivity over the picometer scale of length.

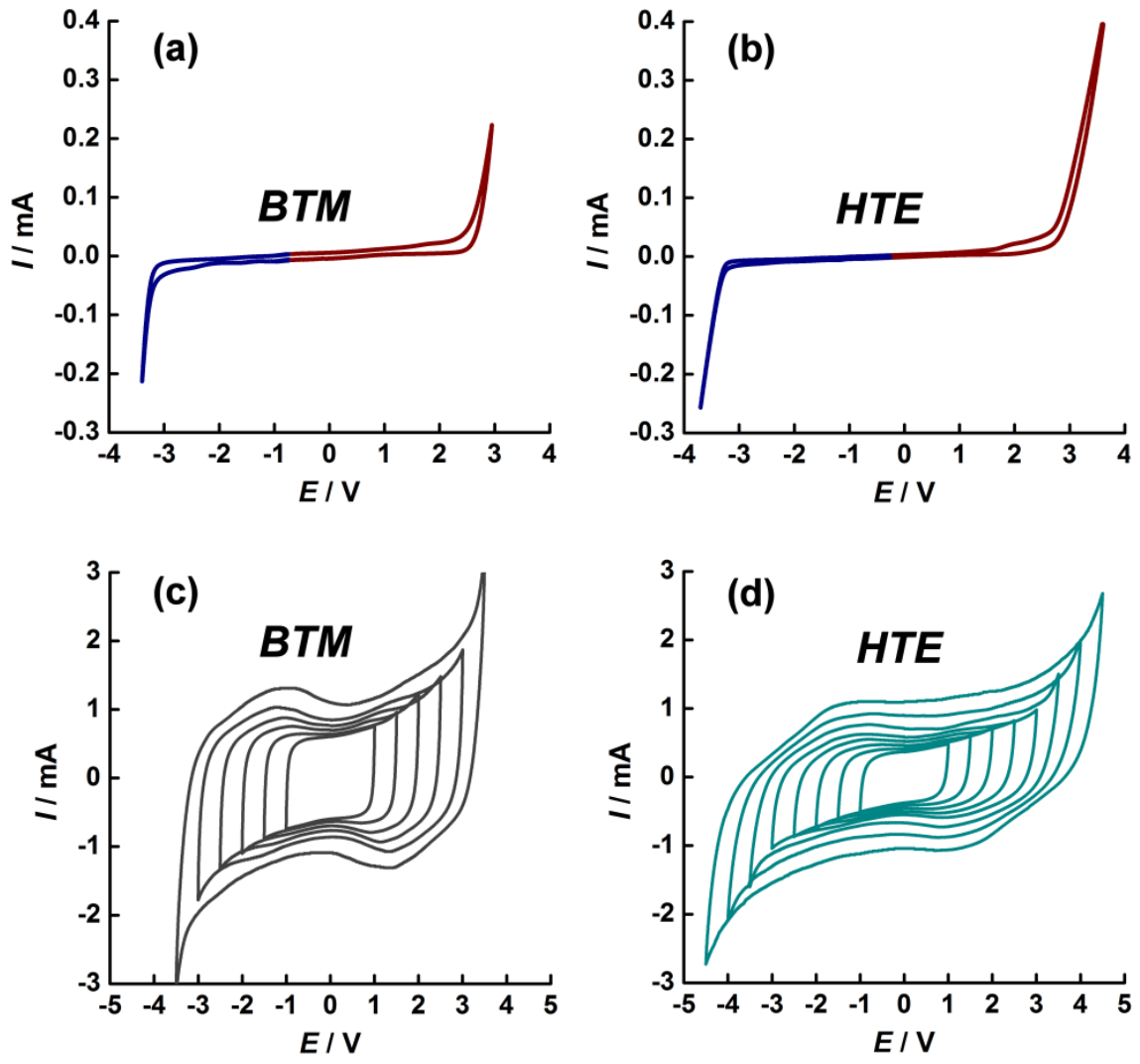

Fig. 3. Voltage Stability Windows of "Quantum-inert" Ionic Liquids at *T*=25°C.

(Top) Cyclic voltammograms recorded at 100 mV s^{-1}. Cathodic and anodic scans recorded separately. The working electrode was a glassy carbon disk (*d* = 3.0 mm) press-fitted into a glass-filled Teflon shroud. The reference half-cell was Ag|AgCl|($TFSI^-$). (a) Butyltrimethylammonium bis(trifluoromethylsulfonyl)imide (BTM). (b) Hexyltriethylammonium bis(trifluoromethylsulfonyl)imide (HTE). In both cases the ionic liquids were driven to decomposition at each voltage limit. The slightly "flatter" response of HTE compared with BTM is caused by the greater solution resistance (by a factor of approximately 2.5). (Bottom) Electric current versus cell voltage for supercapacitors based on (100 μm × 1 cm^2) layers of activated carbon in the corresponding ionic liquid. Scan rate 10 mV s^{-1}. The two-electrode voltage stability windows are >7 V. (c) Butyltrimethylammonium bis(trifluoromethylsulfonyl)imide (BTM). (d) Hexyltriethylammonium bis(trifluoromethylsulfonyl)imide (HTE). A voltammogram of HTE has previously been reported by Sun et al. [29].

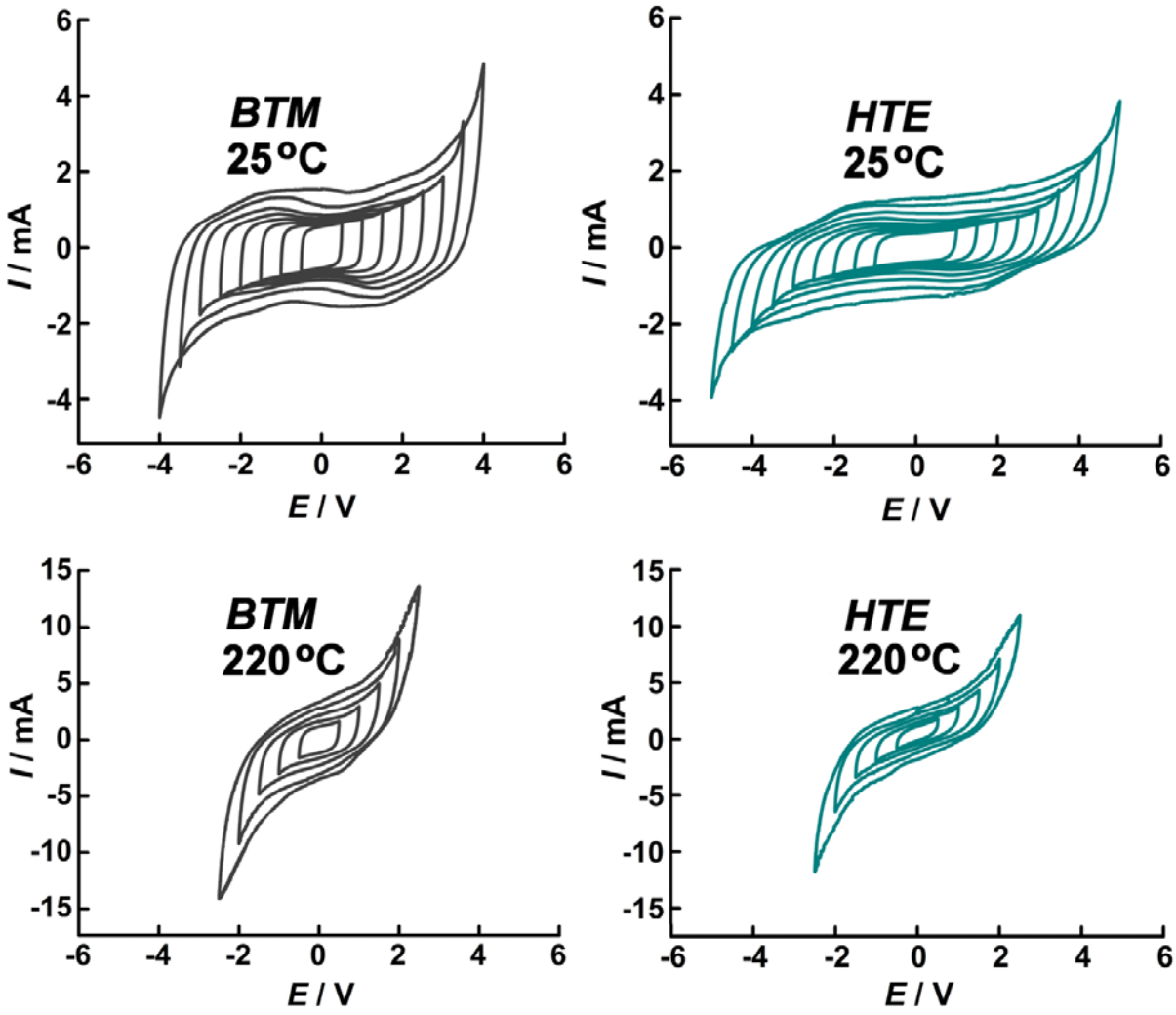

Fig. 4. Voltage Stability Windows of "Quantum-inert" Ionic Liquids in functioning supercapacitors: The Effect of Temperature.

(Left) Butyltrimethylammonium bis(trifluoromethylsulfonyl)imide (BTM). (Right) Hexyltriethylammonium bis(trifluoromethylsulfonyl)imide (HTE). Scan rate 10 mV s^{-1}. The width of the voltage stability window diminishes by a factor of approximately half as the temperature is raised from T=25°C to T=220°C.

Conductivity Results

It has long been recognized that a reciprocal relation exists between ionic conduction and liquid viscosity. The origin of the reciprocity lies in the fact that the motion of an ion through a stationary liquid may also be viewed as the flow of a liquid around a stationary ion. This kinetic equivalence underpins the classical Stokes-Einstein relation, and explains why the activation energy for ionic conduction is the same as the activation energy for viscous flow.

The *thermodynamic* modeling of glasses, however, presents special problems. A glass contains mobility-locked states. Furthermore, these mobility-locked states become unlocked at a characteristic temperature (T_{g}) and pressure (P_{g}) known as the glass transition point. Accordingly, there are four macroscopic degrees of freedom, two external (T, P) and two internal ($T_{\mathrm{g}}, P_{\mathrm{g}}$). The usual choice of thermodynamic potential for physico-chemical problems, the Gibbs Potential, is therefore inadequate in this case because it recognizes only the two external degrees of freedom (T, P).To overcome this difficulty, we here define a new potential

$$\chi = G - G_{\mathrm{g}} \tag{4}$$

where the symbol G indicates the Gibbs function, and the symbol G_{g} indicates the specific value of the Gibbs function at the glass transition point. Hereafter, we refer to the potential χ (chi) as the *thermodynamic difference potential* or, more prosaically, as the *thermodynamic difference energy*.

The main advantage of working with χ is that, at constant temperature and pressure of a surrounding heat bath, its differential takes a particularly simple form, *viz*.

$$\Delta\chi = \Delta\left(U - U_{\mathrm{g}}\right) - \left(T - T_{\mathrm{g}}\right)\Delta S_{\mathrm{sys}} + \left(P - P_{\mathrm{g}}\right)\Delta V_{\mathrm{sys}} \tag{5}$$

Here U is the internal energy of the system, S_{sys} is the entropy of the system, and V_{sys} is the volume of the system.

In order for an ion to become mobile, it must acquire a minimum amount of energy, called the activation energy. Based on the above definitions, direct modeling of the activation energy can be achieved by means of the Boltzmann Relation. The latter has long been used to link classical thermodynamics with kinetics. Here we apply it in the standard form:

$$\kappa = \kappa_{\infty}\exp\left(\frac{\Delta S_{\mathrm{T}}^{*}}{k_{\mathrm{B}}}\right) \tag{6}$$

where κ is the conductivity $(\mathrm{S\ m^{-1}})$, κ_∞ is the limiting conductivity $(\mathrm{S\ m^{-1}})$ at infinitely high temperature, S_T is the total entropy of the system and surrounding heat bath, and the asterisk refers to the transition state. By noting that

$$\Delta S_\mathrm{T} = \Delta S_\mathrm{sys} + \Delta S_\mathrm{bath} \tag{7}$$

Then combination of Eq. (5), Eq. (6) and Eq. (7) soon yields

$$\kappa = \kappa_\infty \exp\left(\frac{-\Delta\chi^*}{k_\mathrm{B}(T - T_\mathrm{g})}\right) \tag{8}$$

This equation has the same outward form as the celebrated (but wholly empirical) Vogel-Tammann-Fulcher equation [10–12] and can therefore be regarded as a rigorously-derived version of it. It also reveals something new: the activation energy which appears in Eq. (8) is not the usual Gibbs energy but the *thermodynamic difference energy* defined by Eq. (4). Thus, the activation energy turns out to be the energy required to unlock the mobile states at temperatures above the glass transition temperature T_g. It is also pleasing to note that if $T_g = 0$ then the empirical Arrhenius expression is recovered.

Over the past half century, various forms of the Vogel-Tammann-Fulcher equation have been applied to the conductivity (and viscosity) of softened glasses, and in 2006 the equation was applied to the conductivity of some ionic liquids by Vila et al. [40]. However, despite its widespread adoption, no consensus has been reached regarding a microscopic model of the activation energy. Various models have been proposed, of varying degrees of complexity, but none has achieved universal acceptance. Well-known examples include the free volume model of Cohen and Turnbull [41] and the configurational entropy model of Adam and Gibbs [42]. In the free volume model, it is assumed that the activation energy arises from the work to form small voids in the softened glass; while in the configurational entropy model, it is assumed that the activation energy depends inversely on the number of structural configurations available to the softened glass. In the present work we propose a radically different model for the activation energy. We suggest that the activation energy arises from the change in internal energy required to detach the mobile species from its glass matrix. Thus,

$$\Delta\chi^* \approx \Delta\left(U - U_\mathrm{g}\right) \tag{9}$$

Strong evidence in favor of this idea is that estimates of the glass transition temperature obtained by the VTF method and by the DSC method coincide within experimental error (**Table 2**).

Table 2. Parameterization of plots of $\ln\kappa - \ln\kappa_\infty$ *versus* $T_g/(T_g - T)$.

Code	Ionic Liquid	Gradient ($N/2$)	Intercept κ_∞/S m^{-1}	T_g/K (VTF)	T_g/K (DSC)	T_g/K (Shock Cooling)
● BTM	Butyltrimethylammonium bis(trifluoromethylsulfonyl)imide	3.27	0.208	187±5	195±5	185±5
● HTE	Hexyltriethylammonium bis(trifluoromethylsulfonyl)imide	3.65	0.208	190±5	188±5	195±5

Further progress can now be made based on a microscopic model. Our reasoning may be summarized as follows. (i) The rate-determining step for ionic conduction is the detachment of the mobile species from its glass matrix. (ii) The same rate-determining step controls the glass transition at (T_g, P_g). (iii) The glass-to-liquid transition at (T_g, P_g) is always endothermic. (iv) The endothermicity is due to a "late" transition state (the Hammond Postulate) [43]. (v) The existence of a "late" transition state implies that the change in internal energy is due to the work of detachment and equilibration of the mobile species. (vi) For weakly cohesive glasses, the work of detachment and equilibration is simply the energy needed to activate the N new degrees of freedom of the mobile species at (T_g, P_g). (vii) By the equipartition of energy, each new degree of freedom of the mobile species requires $k_B T_g/2$ of kinetic energy to be activated at (T_g, P_g). Combining all these assumptions, the activation energy for ionic conduction becomes

$$\Delta\chi^* \approx p + N\frac{k_B T_g}{2} \tag{10}$$

where p is the energy of cohesion. Further, if the constituent ions of the glass are weakly associated, then $p \ll N(k_B T_g/2)$, and

$$\kappa \approx \kappa_\infty \exp\left(\frac{N}{2}\frac{T_g}{T_g - T}\right) \tag{11}$$

In this limit, plots of $\ln(\kappa)$ versus $T_g/(T_g - T)$ should yield straight lines having slopes $N/2$ and intercepts $\ln(\kappa_\infty)$. Some examples are shown in **Fig. 5**.

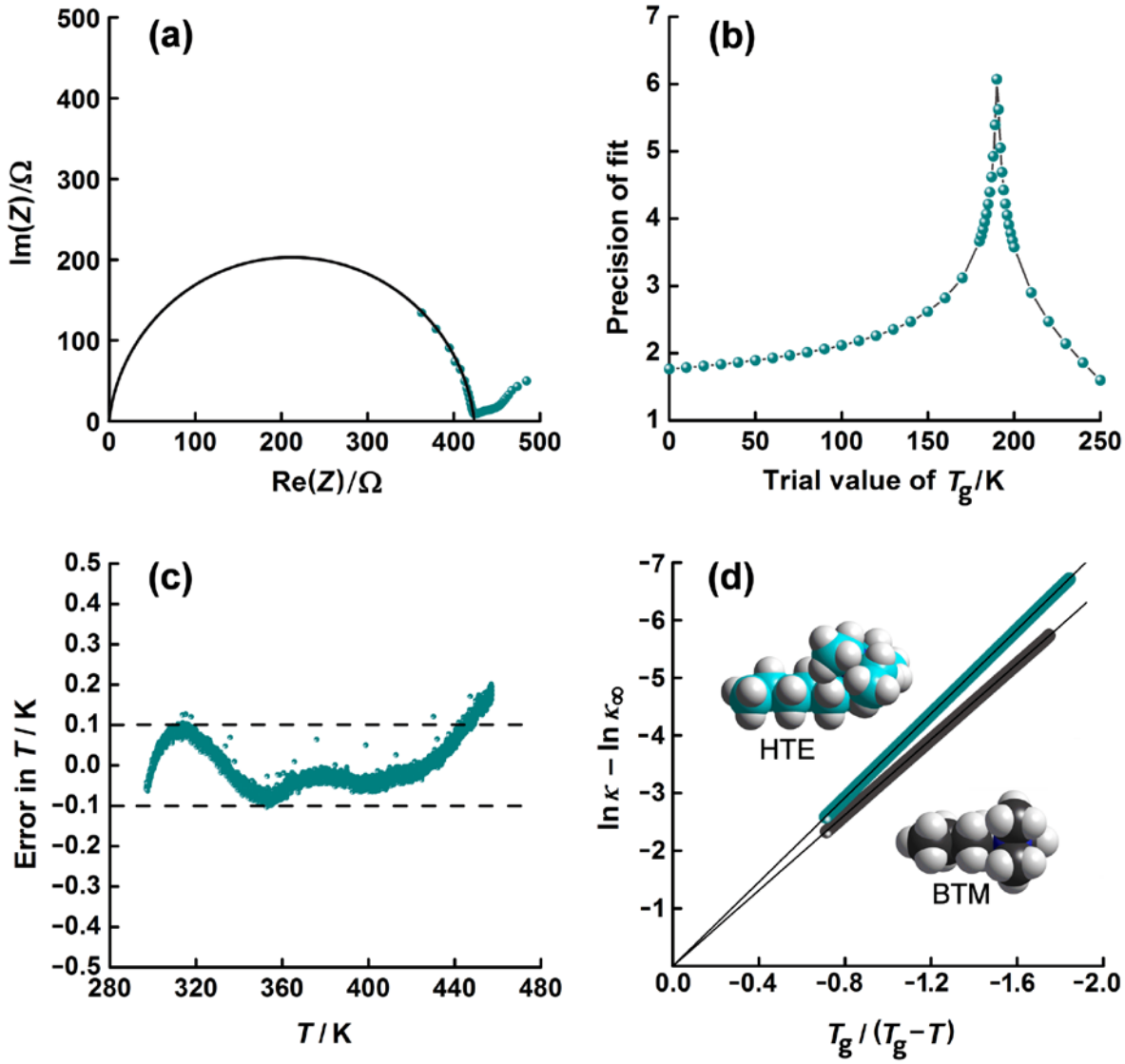

Fig. 5. Very High Precision Conductivity Measurements of Ionic Liquids.

(a) The AC impedance response of two platinized platinum electrodes in butyltrimethylammonium bis(trifluoromethylsulfonyl)imide at 25 ˚C. Data obtained using a Jenway conductivity probe (027-013) coupled to a Wayne-Kerr Bridge (6430A). The local minimum is observed at 10 kHz, where the phase angle $\theta < 2$ degrees. The resistance may be calculated from the equation $R = Z_{\text{real}}(1 + \tan^2\theta)$.

(b) A plot of precision-of-fit of Eq. (8) versus trial values of T_g for hexyltriethylammonium bis(trifluoromethylsulfonyl)imide. Precision-of-fit is measured as $-\log(1 - R^2)$, where R is the Pearson product-moment correlation co-efficient. The most precise fit occurs at $T_g = 190\ \text{K}$, which corresponds within experimental error to the glass transition temperature of this ionic liquid. (Note. The precision-of-fit as defined here measures the "number-of-nines" of the correlation coefficient R^2.)

(c) Systematic error in the fitting of the Vogel–Tammann–Fulcher (VTF) equation to high precision conductivity data, expressed as equivalent temperature error. The data imply that the VTF relation holds within $\pm 0.1\ \text{K}$ over the range 300 K to 450 K. Note that, at the lower

end of the temperature range, large dispersions of local viscosity and local temperature occur, so that very slow ramp speeds (timescale of hours) are needed to obtain uniform conditions.

(d) Plots of $\ln\kappa - \ln\kappa_\infty$ versus $T_g/(T_g - T)$ for butyltrimethylammonium bis(trifluoromethylsulfonyl)imide (BTM) and hexyltriethylammonium bis(trifluoromethylsulfonyl)imide (HTE). Approx. 40,000 data points per plot.

Interestingly, Eq. (11) corresponds precisely to an empirical equation of Angell [44], *viz*.

$$\kappa \approx \kappa_\infty \exp\left(\frac{DT_g}{T_g - T}\right) \tag{12}$$

where D is an empirical constant, commonly referred to as the "fragility" of the glass. Based on the present work, we can now identify this constant as $N/2$, where N is the number of new degrees of freedom that are created by the detachment of the mobile species from the glass matrix. We also observe that the wide applicability of Angell's Equation (11) is a direct consequence of the wide applicability of the Equipartition Principle.

Elementary geometric considerations suggest a universal minimum value of 6 for the parameter N. This is predicted in the case of a non-associated, non-linear, polyatomic mobile species having three translational degrees of freedom and just three rotational degrees of freedom. Although the quaternary ammonium ions used in the present work actually approach this value, we have found that their N values are slightly higher, in the range 6–8, most likely because the charged nature of the ions causes some inter-ionic (cohesive) association. We note, however, that a value of precisely 6 has been reported in the case of *o*-terphenyl [45], which has been described by Debenedetti and Stillinger as "the canonical fragile glass-former" [46].

Conclusion

In electrochemistry, both theory and experiment indicate that the rate of electron tunneling decays exponentially with distance between the electrode surface and the acceptor orbital of the reactant species. In the present work, we have discovered that long-chain alkyl groups provide effective shielding of quaternary ammonium cations against this process. This insight has permitted the synthesis of ionic liquids having extreme chemical inertness. Shock cooling of these same ionic liquids, followed by re-heating, has also led to the discovery that the critical temperature for the onset of bulk conductivity coincides with the glass transition temperature (Table 2). An immediate corollary is that the ionic liquids used in the present work are actually softened glasses at temperatures in the supercooling range. Finally, the fact that the

conductivity of ionic liquids can be measured over very wide ranges of temperature (more than 150°C) has allowed the fitting of the Vogel-Tammann-Fulcher equation to "six nines" precision (R^2 > 0.999999). This achievement, in turn, has permitted the glass transition temperature to be estimated within ± 5°C, a result comparable with the best thermal methods.

Acknowledgements

Dr. Pik Leung Tang is thanked for assistance with DSC measurements. This work was financially supported by Schlumberger WCP Ltd (U.K.) and E.P.S.R.C. (U.K.).

References

[1] Gabriel S and Weiner J (1888). *Ueber einige Abkömmlinge des Propylamins*. Berichte der deutschen chemischen Gesellschaft, 21 (2): 2669–2679

[2] Plechkova NV and Seddon KR (2008). *Applications of ionic liquids in the chemical industry*. Chem. Soc. Rev., 37: 123–150

[3] Maase M and Massonne K (2005). *Biphasic Acid Scavenging Utilizing Ionic Liquids: The First Commercial Process with Ionic Liquids. Ionic Liquids IIIB: Fundamentals, Progress, Challenges, and Opportunities. Transformations and Processes.* Eds: Rogers RD, Seddon KR. Pub: American Chemical Society. Chapter 10, pp 126–132

[4] Mohammad A (Editor), Dr. Inamuddin (Editor) (2012) *Green Solvents II. Properties and Applications of Ionic Liquids*. Springer (Dordrecht; New York)

[5] Sheldon R (2001) *Catalytic reactions in ionic liquids*, Chem. Commun., 2399–2407

[6] Swatloski RP, Holbrey JD and Rogers RD (2003) *Ionic liquids are not always green: hydrolysis of 1-butyl-3-methylimidazolium hexafluorophosphate.* Green Chem., 5: 361–363

[7] Endres F (2010) *Physical chemistry of ionic liquids*. Phys. Chem. Chem. Phys., 12: 1648–1648

[8] Katayama Y (2011) *General Techniques*, in *Electrochemical Aspects of Ionic Liquids*, Second Edition (Ed. H. Ohno), John Wiley & Sons, Inc., Hoboken, NJ, USA. pp 33–42

[9] Appetecchi GB, Montanino M, Carewska M, Moreno M, Alessandrini F, and Passerini *S* (2011) *Chemical–physical properties of bis(perfluoroalkylsulfonyl)imide-based ionic liquids.* Electrochimica Acta, 56: 1300–1307

[10] Vogel H (1921) Das Temperatur-abhängigkeitsgesetz der Viskosität von Flüssigkeiten, *Physik. Z.* 22: 645−646

[11] Tammann G, Hesse W (1926) Die Abhängigkeit der Viscosität von der Temperatur bei unterkühlten Flüssigkeiten. *Z. Anorg. Allg. Chem*. 156: 245–257

[12] Fulcher GS (1925) Analysis of recent measurements of the viscosity of glasses. *J. Am. Ceramic Soc*. 8: 339–355

[13] Atkin R and Warr GG (2007) *Structure in Confined Room-Temperature Ionic Liquids*. J. Phys. Chem. C, 111 (13): 5162–5168

[14] Mezger M, Schröder H, Reichert H, Schramm S, Okasinski JS, Schöder S, Honkimäki V, Deutsch M, Ocko BM, Ralston J, Rohwerder M, Stratmann M, Dosch H (2008) *Molecular Layering of Fluorinated Ionic Liquids at a Charged Sapphire (0001) Surface.* Science 322: 424–428

[15] Waldmann T, Huang H-H, Hoster HE, Höfft O, Endres F, and Behm RJ (2011) *Imaging an Ionic Liquid Adlayer by Scanning Tunneling Microscopy at the Solid|Vacuum Interface.* ChemPhysChem 12: 2565–2567

[16] Atkin R, Borisenko N, Drüschler M, El Abedin SZ, Endres F, Hayes R, Huber B, and Roling B (2011) *An in situ STM /AFM and impedance spectroscopy study of the extremely pure 1-butyl-1-methylpyrrolidinium tris(pentafluoroethyl)trifluorophosphate/Au(111) interface: potential dependent solvation layers and the herringbone reconstruction*. Phys. Chem. Chem. Phys.,13: 6849–6857

[17] Roling B, Drüschler M, Huber B (2012) *Slow and fast capacitive process taking place at the ionic liquid/electrode interface*. Faraday Discuss. 154: 303–311

[18] Kilic MS, Bazant MZ, Ajdari A (2007) *Steric effects in the dynamics of electrolytes at large applied voltages. I. Double-layer charging.* Phys. Rev. E, 75 Article 021502

[19] Fedorov MV and Kornyshev AA (2008) *Ionic Liquid Near a Charged Wall: Structure and Capacitance of Electrical Double Layer.* J. Phys. Chem. B, 112: 11868–11872

[20] Paek E, Pak AJ, and Hwang GS (2013) *A Computational Study of the Interfacial Structure and Capacitance of Graphene in [BMIM][PF6] Ionic Liquid.* J. Electrochem. Soc. 160, (1) A1-A10 doi: 10.1149/2.019301jes

[21] *Chemfiles Enabling Technologies: Ionic Liquids*. (2005). Pub by Sigma-Aldrich Co., 5 (6) page 2.

[22] Gordon CM, Holbrey JD, Kennedy AR and Seddon KR (1998) *Ionic liquid crystals: hexafluorophosphate salts.* J. Mater. Chem., 8: 2627–2636

[23] Holbrey JD and Seddon KR (1999) *The phase behaviour of 1-alkyl-3-methylimidazolium tetrafluoroborates; ionic liquids and ionic liquid crystals.* J. Chem. Soc., Dalton Trans., 2133–2140 DOI: 10.1039/A902818H

[24] Binnemans K (2005) *Ionic Liquid Crystals*. Chem. Rev., 105: 4148–4204

[25] Mushrush GW and Hazlett RN (1984) *Pyrolysis of Organic Compounds Containing Long Unbranched Alkyl Groups.* Ind. Eng. Chem. Fundam. 23: 288–294

[26] McNaught AD and Wilkinson A (1997) *IUPAC Compendium of Chemical Terminology*, 2nd ed. Blackwell Scientific Publications, Oxford

[27] Snook GA, Best AS, Pandolfo AG, and Hollenkamp AF (2006) *Evaluation of a Ag|Ag+ reference electrode for use in room temperature ionic liquids.* Electrochemistry Communications, 8(9): 1405–1411

[28] Tokuda H, Tsuzuki S, Hasan MAB, Hayamizu SK, Watanabe MJ (2006) How Ionic Are Room-Temperature Ionic Liquids? An Indicator of the Physicochemical Properties. *J. Phys. Chem. B*. 110: 19593–19600

[29] Sun J, Forsyth M, MacFarlane DR (1998) Room-Temperature Molten Salts based on the Quaternary Ammonium Ion. *J. Phys. Chem. B*. 102: 8858–8864

[30] Roberts NJ, Seago A, Carey JS, Freer R, Preston C, Lye GJ (2004) Lipase catalysed resolution of the Lotrafiban intermediate 2,3,4,5-tetrahydro-4-methyl-3-oxo-1H-1,4-benzodiazepine-2-acetic acid methyl ester in ionic liquids: comparison to the industrial *t*-butanol process. *Green Chem*. 6: 475–482

[31] Wei D, Ng TW (2009) Application of novel room temperature ionic liquids in flexible supercapacitors. *Electrochemistry Communications* 11: 1996–1999

[32] Stewart JJP (1989) Optimization of Parameters for Semi-empirical Methods I. Method. *J. Computational Chem.* 10: 209−220

[33] Fletcher S (2010) The Theory of Electron Transfer. *Journal of Solid State Electrochemistry* 14: 705–739

[34] Levich VG, Dogonadze RR (1959), Theory of Non-Radiative Electronic Transitions between Ions in Solution. *Doklady Akad Nauk SSSR, Ser. Fiz. Khim.* 124: 123–126. (In Russian)

[35] Slater JC (1930) Atomic Shielding Constants. *Phys. Rev*. 36: 57–64.

[36] Moser CC, Keske JM, Warncke K, Farid RS, Dutton PL (1992) Nature of Biological Electron-Transfer. *Nature* 355: 796–802

[37] Moser CC, Page CC, Farid R, Dutton PL (1995) Biological Electron Transfer. *J. Bioenergetics and Biomembranes* 27: 263–274

[38] Welton T (1999) Room-Temperature Ionic Liquids: Solvents for Synthesis and Catalysis. *Chem. Rev.* 99: 2071−2083

[39] Holbrey JD, Rogers RD (2008) *Physicochemical Properties of Ionic Liquids: Melting Points and Phase Diagrams*, in *Ionic Liquids in Synthesis*, (Vol 1, Ch 3.1, pp 57–71) Ed. by Wasserscheid P, Welton T (Wiley-VCH, Weinheim)

[40] Vila J, Ginés JP, Pico JM, Franjo C, Jiménez E, Varela LM, Cabeza O (2006)Temperature dependence of the electrical conductivity in EMIM-based ionic liquids: Evidence of Vogel-Tammann-Fulcher behavior. *Fluid Phase Equilibria* 242: 141–146

[41] Cohen MH, Turnbull D (1964) Metastability of Amorphous Structures. *Nature* 203: 964

[42] Adam G, Gibbs JH (1965) On the Temperature Dependence of Cooperative Relaxation Properties in Glass-Forming Liquids. *J. Chem. Phys.* 43: 139–146

[43] Hammond GS (1955), A Correlation of Reaction Rates. *J. Am. Chem. Soc*. 77: 334–338

[44] Angell CA, *in* Rubí J-M, Pérez-Vicente C (Eds.) (1997) *Lecture Notes in Physics, Vol. 492. Complex Behaviour of Glassy Systems*. Springer-Verlag (Berlin, Heidelberg, New York)

[45] Greet RJ and Turnbull D (1967) *Glass Transition in o-Terphenyl.* J.Chem. Phys., 46: 1243–1251

[46] Debenedetti PG and Stillinger FH (2001) *Supercooled liquids and the glass transition*. Nature 6825: 259–267

<end>